

Strange Particle Production from SIS up to 40 $A\cdot\text{GeV}$

Helmut Oeschler

Institut für Kernphysik, Darmstadt University of Technology,
D-64289 Darmstadt, Germany

Abstract. A review of strange particle production in heavy ion collisions at incident energies from SIS up to 40 $A\cdot\text{GeV}$ is presented. A statistical model assuming chemical equilibrium and local strangeness conservation (i.e. strangeness conservation per collision) describes most of the observed features.

It is demonstrated that the K^- production at SIS energies occurs predominantly via strangeness exchange and that this channel is approaching chemical equilibrium. The observed maximum in the K^+/π^+ excitation function is also seen in the ratio of strange to non-strange particle production. The appearance of this maximum around 30 $A\cdot\text{GeV}$ is due to the energy dependence of the chemical freeze-out parameters temperature T and baryo-chemical potential μ_B .

Keywords: list of keywords, relevant to the article

PACS: 25.75.-q

1. Introduction

Central heavy ion collisions at relativistic incident energies represent an ideal tool to study nuclear matter at high temperatures. Particle production is – at all incident energies – a key quantity to extract information on the properties of nuclear matter under these extreme conditions. Particles carrying strangeness have turned out to be very valuable messengers. Among the many results obtained so far, only a few observations are discussed together with their interpretations.

- At SIS energies, the measured K^- yields is comparable to the K^+ yield at the same energy relative to the production threshold in NN collisions. This is in clear contrast to elementary reactions.
- The measured ratio K^+/π^+ as a function of incident energy exhibits a maximum around 30 $A\cdot\text{GeV}$. What is the origin of this maximum? Why does the

K^-/π^- ratio rise monotonically without exhibiting a maximum?

Before discussing these points the main differences between K^+ and K^- production and their interaction with nuclear matter are mentioned.

2. Production of pions and kaons

At incident energies around 1 A-GeV pion and kaon production is very different: Pions can be produced by direct NN collisions in contrast to kaons. The threshold for K^+ production in NN collisions is 1.58 GeV and only via collective effects the energy needed to produce a K^+ together with a Λ (or another strange particle due to strangeness conservation) can be accumulated. The threshold for K^- production is even higher (2.5 GeV) as they are produced as $K^+ K^-$ pairs.

The interaction of K^+ and K^- with nuclear matter is also very different. Due to their \bar{s} content K^+ cannot be absorbed, while K^- can easily be absorbed on a nucleon converting it into a Λ . Hence, the K^+ have a small interaction cross section, while π and K^- exhibit large values. Consequently, the K^+ have a long mean free path of about 6 fm, while K^- and π have much shorter ones. This property makes the K^+ ideal messengers of the early stage of the collision to extract information on the stiffness of the nuclear equation of state [1].

3. Interpretation within a statistical model

Pions and K^+ exhibit a further very pronounced contrast: While the pion multiplicity per number of participating nucleons A_{part} remains constant with A_{part} , the K^+ multiplicity per A_{part} rises strongly (Fig. 1). The latter observation seems to be in conflict with a thermal interpretation, which – in a naive view – should give multiplicities per mass number being constant.

Usually, the particle number densities or the multiplicities per A_{part} , here for pions, are described in a simplified way by a Boltzmann factor $\frac{M_\pi}{A_{part}} \sim \exp\left(-\frac{\langle E_\pi \rangle}{T}\right)$ with the temperature T and the total energy $\langle E_\pi \rangle$.

The production of strange particles has to fulfil strangeness conservation. The attempt to describe the measured particle ratios including strange hadrons at AGS, SPS and RHIC using a strangeness chemical potential μ_S is quite successful [3–6]. However, this grand-canonical treatment is not correct if the number of produced strange particles is small. Then a statistical model has to take care of *local strangeness conservation* in each reaction as introduced in [7]. This canonical description is done by taking into account that e.g. together with each K^+ a Λ or another strange particle is produced:

$$\frac{M_{K^+}}{A_{part}} \sim \exp\left(-\frac{\langle E_{K^+} \rangle}{T}\right) \left[g_\Lambda V \int \frac{d^3p}{(2\pi)^3} \exp\left(-\frac{(E_\Lambda - \mu_B)}{T}\right) \right]$$

with T the temperature, μ_B the baryo-chemical potential, g_i the degeneracy factors, V the production volume for making the associate pair (see [8,9]) and E_i the total

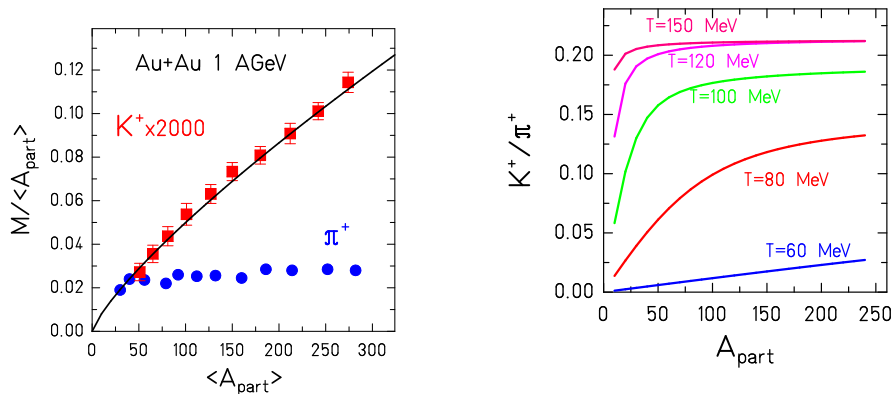


Fig. 1. Left: The multiplicity of K^+ / A_{part} rises strongly with A_{part} in contrast to the pion multiplicity [2]. This rise can be described by the statistical model including local strangeness conservation (see text). Right: Examples of a canonical description for various values of T .

energies. We note that this volume is not identical to the volume of the system at freeze out.

This formula, simplified for demonstration purposes, neglects other combinations leading to the production of K^+ as well as the use of Bose-Fermi distributions, which are all included in the computation. The corresponding formula for K^- production

$$\frac{M_{K^-}}{A_{part}} \sim \exp\left(-\frac{\langle E_{K^-} \rangle}{T}\right) \left[g_{K^+} V \int \frac{d^3p}{(2\pi)^3} \exp\left(-\frac{E_{K^+}}{T}\right) \right]$$

is similar, but does not depend on μ_B . This point will become important later on.

These formulae lead to a reduction of K^+ and K^- yields as compared to the numbers calculated without exact strangeness conservation [8, 9]. Two extreme conditions can be seen from these equations. In the limit of a small number of strange particles the additional term (due to the parameter V) leads to a linear rise of M_{K^+} / A_{part} , while M_{π} / A_{part} remains constant. This is in very good agreement with the experimental observations shown in Fig. 1. For very high temperatures or very large volumina, the terms in brackets approach unity (see Ref. [8]) resulting in the grand-canonical formulation. This is much better seen in the exact formulae using modified Bessel functions [8–10].

At low incident energies, the particle ratios (except η / π_0) are well described using this canonical approach [8]. Surprisingly, even the measured K^+ / K^- ratio is described and this ratio does not depend on the choice of the volume term V .

4. K^+ and K^- yields at SIS energies

Before comparing calculations to data in detail, a summary of the measurements by the KaoS Collaboration is given. These results have attracted considerable interest as in heavy ion collisions the K^- yield compared to the K^+ cross section is much higher than expected from NN collisions [12, 13]. This is especially evident if the kaon multiplicities are plotted as a function of $\sqrt{s} - \sqrt{s_{th}}$ where $\sqrt{s_{th}}$ is the energy needed to produce the respective particle in NN collisions taking into account the mass of the associatedly produced partner. To produce a K^+ in NN collisions $\sqrt{s_{th}} = 2.548$ GeV and a K^- $\sqrt{s_{th}} = 2.87$ GeV. The obvious contrast between NN and AA collisions, shown in Fig. 2, left, has led to the interpretation of the results by in-medium properties which cause e.g. a lower threshold for K^- production when produced in dense matter [14].

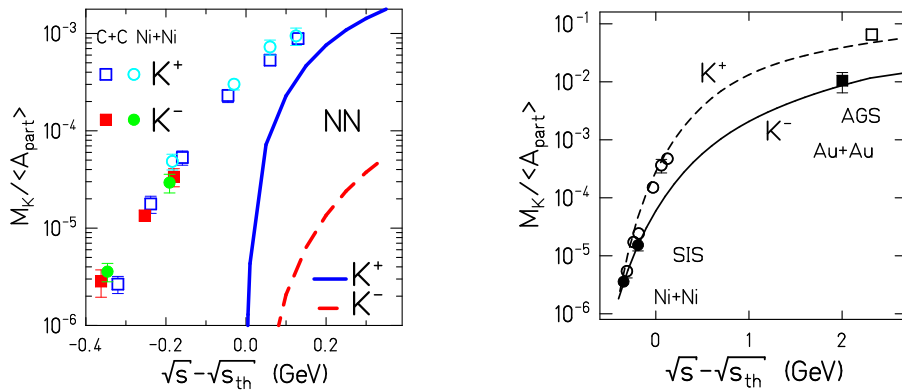


Fig. 2. Left: Measured K^+ and K^- yields in heavy ion (symbols, from [11–13]) and in NN collisions (solid line from a compilation of [19]) as a function of $\sqrt{s} - \sqrt{s_{th}}$. $\langle A_{part} \rangle$ is $A/2$ for heavy ion data and 2 for NN collisions. Right: Calculated K^+/A_{part} and K^-/A_{part} ratios in the statistical model as a function of $\sqrt{s} - \sqrt{s_{th}}$ for Ni+Ni collisions. The points are results for Ni+Ni collisions at SIS energies [11, 13] and Au+Au at 10.2 A -GeV (AGS) [16]. At AGS energies the influence of the system mass is negligible.

It is therefore of interest to see how the results of the statistical model appear in a representation where the K^+ and the K^- multiplicities are given as a function of $\sqrt{s} - \sqrt{s_{th}}$. Figure 2, right demonstrates that at values of $\sqrt{s} - \sqrt{s_{th}}$ less than zero the excitation functions for K^+ and K^- cross leading to the observed equality of K^+ and of K^- at SIS energies. The yields differ at AGS energies by a factor of five. The difference in the rise of the two excitation functions can be understood by the formulae given above. The one for K^+ production contains $(E_\Lambda - \mu_B)$ while the other has E_{K^+} in the exponent of the second term. As these two values are

different, the excitation functions, i.e. the variation with T , exhibit a different rise.

Furthermore, the two formulae predict that the K^+/K^- ratio for a given collision should not vary with the centrality as the volume V cancels in the ratio. This has indeed been observed in Au+Au/Pb+Pb collisions between 1.5 A·GeV and RHIC energies [11, 15–18] as shown in Fig. 3. This independence of centrality is most astonishing as one expects at low incident energies an influence of the different thresholds and the density variation with centrality. For instance at 1.93 A·GeV the K^+ production is above and the K^- production below their respective NN thresholds.

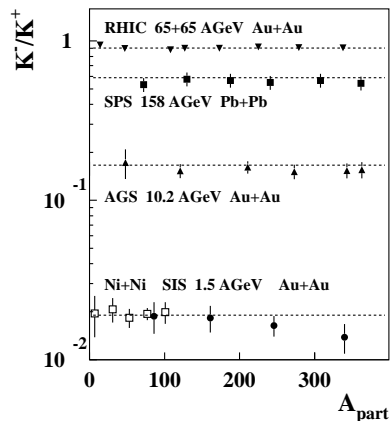


Fig. 3. The K^+/K^- ratio appears to be constant of a function of centrality from SIS up to RHIC energies. The dotted lines represent the predictions of the statistical model. Data from [11, 16, 17].

Transport-model calculations clearly show that strangeness equilibration requires a time interval of 40 – 80 fm/c [20, 21]. On the other hand statistical models assuming chemical equilibration are quite successful in describing the particle yields including strange particles.

In the case of K^+ production, no strong absorptive channel seems to be available which could lead to chemical equilibration. For K^- production the situation is quite different. At low incident energies strange quarks are found only in a few hadrons. The \bar{s} quark is essentially only in K^+ , while the s quark will be shared between K^- and Λ (or other hyperons). This sharing of the s quark might be in chemical equilibrium as the reactions

$$\pi^0 + \Lambda \rightleftharpoons p + K^- \quad \text{or} \quad \pi^- + \Lambda \rightleftharpoons n + K^-$$

are strong and have a small Q-values of ± 176 MeV.

The idea that the K^- yield is dominated by strangeness exchange via the $\pi^- + \Lambda$ channel has been suggested by [22] and has been demonstrated quantitative

in a recent theoretical study [23]. This study showed that the pair production via direct BB collisions happens early around ≈ 6 fm/c and dies out soon. The strangeness exchange process dominates and has its highest rate around 13 fm/c. The absorption of K^- is very strong and causes that the early produced K^- are not leaving the reaction zone. In contrast, the K^+ production occurs quite early (≈ 7 fm/c) when the highest densities are reached. Therefore, the yield of K^+ is sensitive to the stiffness of the nuclear equation of state [1, 24]. The K^- emission happens later around ≈ 14 fm/c when the density has dropped nearly to about saturation density ρ_0 .

This scenario has consequences which can be tested experimentally. The dominance of the strangeness exchange channel causes a direct correlation of the K^- production to the K^+ yield. This is demonstrated in Fig. 4 showing the multiplic-

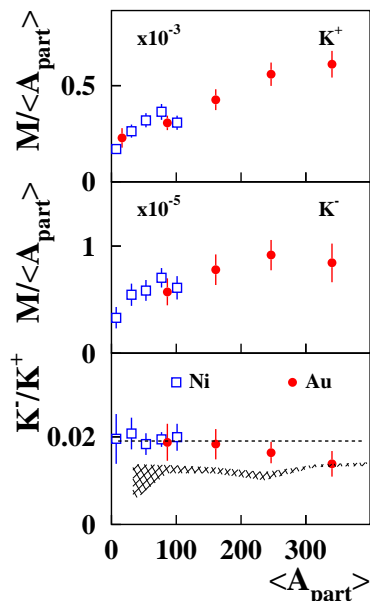


Fig. 4. Multiplicity per A_{part} of K^+ (upper part) and of K^- (middle part) as a function of A_{part} both for Ni+Ni (open squares) and Au+Au (full circles) at a beam energy of 1.5 A-GeV. The lower part exhibits the ratio of the K^-/K^+ which is nearly constant as a function of A_{part} and equal for both systems. The dashed line represents the results of statistical model calculation [8, 9] and the crosshatched area corresponds to IQMD calculations [23]. Data are from [15].

ities of both K^- and K^+ per A_{part} as a function of A_{part} . They exhibit the same rising trend with A_{part} . Consequently, the ratio K^-/K^+ is nearly constant [15]. Model predictions are given as dashed line (statistical model [9]) and crosshatched area (IQMD [23]). It has been shown that this constancy can be interpreted by applying the law of mass action for the strangeness-exchange channel [25].

Furthermore, the late K^- emission is in good agreement with the isotropic angular distribution of the K^- emission observed experimentally [15]. The late emission at nearly normal nuclear matter density however reduces the sensitivity of the K^- yield to the strength of the K^-N potential as discussed in [23] and in the following.

Figure 5 shows the azimuthal distribution of K^+ and π^+ for Au+Au collisions at 1.5 A·GeV. The measured values are corrected for the angular resolution of the reaction plane. The data are described by the function $2v_1 \cos(\phi) + 2v_2 \cos(2\phi)$ resulting in values for v_1, v_2 as given in the figure. The values for v_1 are always close to zero as expected for data taken close to mid-rapidity.

Both π^+ and K^+ exhibit a pronounced out-of-plane enhancement. For emitted π^+ it can easily be interpreted as rescattering (and absorption) in agreement with previous observations [26]. This explanation cannot hold easily for K^+ as the mean free path of 5 fm is rather long and will give only a moderate out-of-plane enhancement [27, 29]. It has been explained by the repulsive K^+N interaction [27, 28].

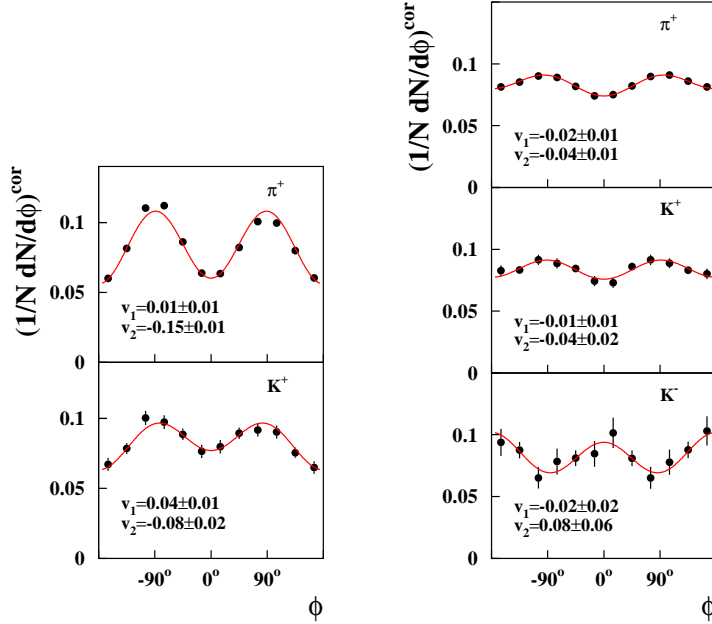


Fig. 5. Left: Measured azimuthal distribution corrected for the resolution of the reaction plane for π^+ and K^+ for semi-peripheral Au+Au collisions at 1.5 A·GeV corresponding to impact parameters between $5.9 \text{ fm} < b < 10.2 \text{ fm}$. The chosen angles refer to rapidities of $0.3 < y/y_{beam} < 0.7$ and the particle momenta are within $0.2 \text{ GeV} < p_t < 0.8 \text{ GeV}$. The lines are fits (see text) resulting in v_1 and v_2 values as given in the figure. Right: Same for Ni+Ni collisions at 1.93 A·GeV corresponding to impact parameters between $3.8 \text{ fm} < b < 6.5 \text{ fm}$ and the same range in rapidity and particle momenta.

The study of Ni+Ni collisions had been performed at the higher incident energy

of 1.93 A·GeV. The higher production cross section for K^- at this energy made it possible to study both kaon species as shown in Fig. 5 together with π^+ . Both π^+ and K^+ follows the trend shown for Au+Au collisions. The v_2 values are smaller as one expect for the smaller system. In striking contrast, the K^- show a rather flat distribution with an indication of even an in-plane enhancement.

The short mean free path of K^- of about 1 fm leads to the expectation of an out-of-plane preference due to absorption. This is clearly not seen. As shown recently, K^- are produced predominantly via the strangeness-exchange reaction which causes both the absorption and production of K^- [15,23]. Consequently, the K^- are emitted later than the K^+ . It might therefore happen that the shadowing spectator has moved away when the emission of K^- occurs. This would lead then to a rather flat distribution, but might hardly lead to an in-plane enhancement. It has been shown that the attractive K^-N interaction will also lead to a flat azimuthal distribution [27,28]. A detailed theoretical study which disentangles this two possible explanation will be published [29].

5. Maximum relative strangeness content in heavy ion collisions around 30 A·GeV

The experimental data from heavy ion collisions show that the K^+/π^+ ratio rises from SIS up to AGS. It is larger for AGS than at the highest CERN-SPS energies [16, 18, 33–35] and decreases even further at RHIC [17]. This behavior is of particular interest as it could signal the appearance of new dynamics for strangeness production in high energy collisions. It was even conjectured that this property could indicate an energy threshold for quark-gluon plasma formation in relativistic heavy ion collisions [36].

In the following we analyze the energy dependence of strange to non-strange particle ratios in the framework of a hadronic statistical model. In the whole energy range, the hadronic yields observed in heavy ion collisions resemble those of a population in chemical equilibrium along a unified freeze-out curve determined by the condition of fixed energy/particle $\simeq 1$ GeV [33] providing a relation between the temperature T and the baryon chemical potential μ_B . As the beam energy increases T rises and μ_B is slightly reduced. Above AGS energies T exhibits only a moderate change and converges to its maximal value in the range of 160 to 180 MeV, while μ_B is strongly decreasing.

Rather than studying the K^+/π^+ ratio we use the ratios of strange to non-strange particle multiplicities (Wroblewski factor) [37] defined as $\lambda_s \equiv \frac{2\langle s\bar{s} \rangle}{\langle u\bar{u} \rangle + \langle d\bar{d} \rangle}$ where the quantities in angular brackets refer to the number of newly formed quark-antiquark pairs, i.e. it excludes all quarks that were present in the target and the projectile.

Applying the statistical model to particle production in heavy ion collisions calls for the use of the canonical ensemble to treat the number of strange particles

particularly for data in the energy range from SIS up to AGS [8] as mentioned before. The calculations for Au-Au and Pb-Pb collisions are performed using a canonical correlation volume defined above. The quark content used in the Wroblewski factor is determined at the moment of *chemical freeze-out*, i.e. from the hadrons and especially, hadronic resonances, before they decay. This ratio is thus not an easily measurable observable unless one can reconstruct all resonances from the final-state particles. The results are shown in Fig. 6 as a function of \sqrt{s} .

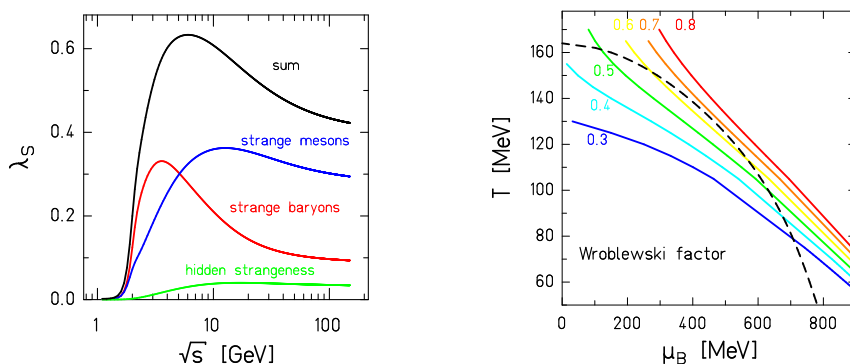


Fig. 6. Left: Contributions to the Wroblewski factor λ_s (for definition see text) from strange baryons, strange mesons, and mesons with hidden strangeness. The sum of all contributions is given by the full line. Right: Lines of constant Wroblewski factor λ_s (for definition see text) in the $T - \mu_B$ plane (solid lines) together with the freeze-out curve (dashed line) [33].

The solid line (marked “sum”) in Fig. 6 describes the statistical-model calculations in complete equilibrium along the unified freeze-out curve [33] with the energy-dependent parameters T and μ_B . From Fig. 6 we conclude that around 30 A-GeV laboratory energy the relative strangeness content in heavy ion collisions reaches a clear and well pronounced maximum. The Wroblewski factor decreases towards higher incident energies and reaches a limiting value of about 0.43. For details see Ref. [38].

The appearance of the maximum can be traced to the specific dependence of μ_B and T on the beam energy. Figure 6 r.h.s. shows lines of constant λ_s in the $T - \mu_B$ plane. As expected λ_s rises with increasing T for fixed μ_B . Following the chemical freeze-out curve, shown as a dashed line in Fig. 6, one can see that λ_s rises quickly from SIS to AGS energies, then reaches a maximum at $\mu_B \approx 500$ MeV and $T \approx 130$ MeV. These freeze-out parameters correspond to 30 A-GeV laboratory energy. At higher incident energies the increase in T becomes negligible but μ_B keeps on decreasing and as a consequence λ_s also decreases.

The importance of finite baryon density on the behavior of λ_s is demonstrated

in Fig. 6 showing separately the contributions to $\langle s\bar{s} \rangle$ coming from strange baryons, from strange mesons and from hidden strangeness, i.e. from hadrons like ϕ and η . As can be seen in Fig. 6, the origin of the maximum in the Wroblewski ratio can be traced to the contribution of strange baryons. This channel dominates at low \sqrt{s} and loses importance at high incident energies. Even strange mesons exhibit a broad maximum. This is due to the presence of associated production of e.g. kaons together with hyperons.

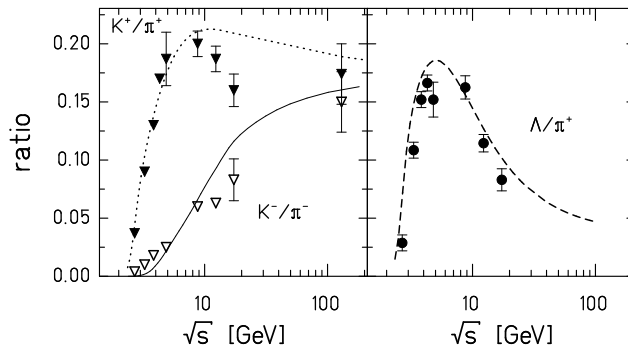


Fig. 7. Ratio of strange–non-strange mesons (left) and Λ/π^+ ratio (right) as a function of \sqrt{s} .

Figure 7 demonstrates nicely the agreement of the statistical model [38] and recent data. As can be understood from the arguments above, the ratio Λ/π exhibit the most pronounced maximum, K^+/π^+ a weaker one and K^-/π^- has no maximum at all. The model gives a good description of the data. It shows a broad maximum in the K^+/π^+ ratio at the same energy as the one seen in the Wroblewski factor. In general, statistical-model calculations should be compared with 4π -integrated results since strangeness does not have to be conserved in a limited portion of phase space. This choice has been made in the data presented in Fig. 7. In contrast to data obtained at midrapidity, a drop in this ratio for 4π yields is seen from preliminary results of the NA49 collaboration at 158 A·GeV [34]. This decrease is, however, not reproduced by the statistical model without further modifications, e.g. by introducing an additional parameter $\gamma_s \sim 0.7$ [39].

6. Summary

Strange particle production in heavy ion collisions over a rather broad range of incident energies can be described by a statistical model. The production of strange particles close to threshold requires a canonical formulation, i.e. explicit strangeness conservation. This approach is able to explain many features of K^+ and K^- production at SIS energies.

While for K^+ production it remains open whether and how chemical equilibrium can be reached, the situation is quite different for K^- . It is shown that the

strangeness exchange process $\pi Y \rightleftharpoons N + K^-$ is the dominant channel for K^- production at SIS and likely also at AGS energies. This is demonstrated by applying the corresponding law of mass action. Theoretical studies confirm this interpretation.

Using the energy dependence of the parameters T and μ_B we have shown that the statistical-model description of relativistic heavy ion collisions predicts that the yields of strange to non-strange particles reaches a well defined maximum near 30 GeV lab energy. It is demonstrated that this maximum is due to the specific shape of the freeze-out curve in the $T - \mu_B$ plane. In particular a very steep decrease of the baryon chemical potential with increasing energy causes a corresponding decline of relative strangeness content in systems created in heavy ion collisions above lab energies of 30 GeV. The saturation in T , necessary for this result, might be connected to the fact that hadronic temperatures cannot exceed the critical temperature $T_c \simeq 170$ MeV for the phase transition to the QGP as found in solutions of QCD on the lattice.

In spite of the apparent success of the statistical models, the impression should not appear that these models describe everything. They describe yields and particle ratios. Looking at spectral shapes already the expansion dynamics shows up. The distribution of the particles in space is a very informative quantity and its description is beyond statistical models.

Acknowledgement(s)

It is a pleasure for me to thank for the stimulating collaboration with J. Aichelin, P. Braun-Munzinger, J. Cleymans, C. Hartnack, K. Redlich, and the whole KaoS Crew (I. Böttcher, A. Förster, E. Grosse, P. Koczoń, B. Köhlmeier, S. Lang, F. Laue, M. Menzel, L. Naumann, M. Płoskoń, F. Pühlhofer, A. Schmah, T. Schuck, E. Schwab, P. Senger, Y. Shin, H. Ströbele, F. Uhlig, A. Wagner, W. Waluś).

References

1. C. Sturm et al., (KaoS Collaboration), Phys. Rev. Lett. **86** (2001) 39.
2. M. Mang, Ph.D.Thesis, University of Frankfurt, 1997.
3. J. Cleymans and H. Satz, Z. Phys. **C57** (1993) 135.
4. P. Braun-Munzinger, J. Stachel, J.P. Wessels and N. Xu, Phys. Lett. B **344** (1995) 43; Phys. Lett. B **365** (1996) 1.
5. P. Braun-Munzinger, I. Heppe, J. Stachel, Phys. Lett. B **465** (1999) 15.
6. P. Braun-Munzinger, D. Magestro, K. Redlich, J. Stachel, Phys. Lett. B **518** (2001) 41.
7. R. Hagedorn, CERN Yellow Report 71-12 (1971); E. Shuryak. Phys. Lett. **B42** (1972) 357; J. Rafelski, Phys. Lett. **B97** (1980) 297; R. Hagedorn et al., Z. Phys. **C27** (1985) 541.
8. J. Cleymans, H. Oeschler, K. Redlich, Phys. Rev. **C59** (1999) 1663.
9. J. Cleymans, H. Oeschler, K. Redlich, Phys. Lett. **485** (2000) 27.

10. J. S. Hamieh, K. Redlich and A. Tounsi, Phys. Lett. **B486** (2000) 61.
11. M. Menzel et al., (KaoS Collaboration), Phys. Lett. **B495** (2000) 26; Ph.D.Thesis, Universität Marburg, 2000.
12. F. Laue, C. Sturm et al., (KaoS Collaboration), Phys. Rev. Lett. **82** (1999) 1640.
13. R. Barth et al., (KaoS Collaboration), Phys. Rev. Lett. **78** (1997) 4007.
14. W. Cassing et al., Nucl. Phys. **A614** (1997) 415.
15. A. Förster, F. Uhlig et al., (KaoS Collaboration), Phys. Rev. Lett. **91** (2003) 152301.
16. L. Ahle et al., (E-802 Collaboration), Phys. Rev. **C58** (1998) 3523; Phys. Rev. **C60** (1999) 044904; L. Ahle et al., E866/E917 Collaboration, Phys. Lett. **B476** (2000) 1; Phys.Lett. **B490** (2000) 53.
17. J. Harris, (STAR Collaboration), Talk presented at QM2001, Stony Brook, January 2001, Nucl. Phys. **A698** 64c.
18. J.C. Dunlop and C.A. Ogilvie, Phys. Rev. **C61** (2000) 031901 and references therein; C. A. Ogilvie. Talk presented at QM2001, Stony Brook, January 2001, Nucl. Phys. **A 698** 3c; J.C. Dunlop, Ph.D.Thesis, MIT, 1999.
19. A. Sibirtsev, W. Cassing and C.M. Ko, Z. Phys. **A358** (1997) 101.
20. P. Koch, B. Müller and J. Rafelski, Phys. Rep. **142** (1986) 167.
21. E.L. Bratkovskaya et al., Nucl. Phys. **A675** (2000) 661.
22. C. M. Ko, Phys. Lett. **B138** (1984) 361.
23. C. Hartnack, H. Oeschler, J. Aichelin, Phys. Rev. Lett. **90** (2003) 102301.
24. C. Fuchs et al., Phys. Rev. Lett. **86** (2001) 1974.
25. H. Oeschler, J. Phys. G: Nucl. Part. Phys. **27** (2001) 1.
26. D. Brill et al., (KaoS Collaboration), Phys. Rev. Lett. **71** (1993) 336; Z. Phys. **A 355** (1996) 61; Z. Phys. **A 357** (1997) 207.
27. Li et al., Phys. Lett. **B 381** (1996) 17.
28. Z.S. Wang et al., EPJ **A5** (1999)275.
29. C. Hartnack et al., to be published.
30. A. Tounsi and K. Redlich, Eur. Phys. **J C24** (2002) 589.
31. E. Andersen, et al. (WA97 Coll.), Phys. Lett. **B449** (1999) 401.
32. N. Carrer (NA57 Coll.), in Proceedings of QM2001.
33. J. Cleymans and K. Redlich, Phys. Rev. Lett. **81** (1998) 5284; Phys. Rev. **C60** (1999) 054908.
34. Ch. Blume, NA49 Collaboration. Talk presented at QM2001, Stony Brook, January 2001, Nucl. Phys. **A 698** (2001) 104c.
35. I. Bearden et al., (NA44 Collaboration), Phys. Lett. **B471** (1999) 6.
36. M. Gaździcki and M. Gorenstein, Acta Phys. Pol. **B30** (1999) 2705; M. Gaździcki and D. Röhrich, Z. Phys. **C71** (1996) 55.
37. A. Wroblewski, Acta Physica Polonica **B16** (1985) 379.
38. P. Braun-Munzinger, J. Cleymans, H. Oeschler, K. Redlich, Nucl. Phys. **A 697** (2002) 902.
39. F. Becattini, J. Cleymans, A. Keränen, E. Suhonen and K. Redlich, Phys. Rev. **C64** (2001) 024901.